

# MOLTEN SALT PHASE DIAGRAMS CALCULATION USING ARTIFICIAL NEURAL NETWORK OR PATTERN RECOGNITION-BOND PARAMETERS<sup>①</sup>

## Part 1. The prediction of the phase diagrams of binary molten salt systems

Wang Xueye, Qiu Guanzhou and Wang Dianzuo

*Department of Mineral Engineering, Central South University of Technology,  
Changsha 410083, P. R. China*

Chen Nianyi

*Shanghai Institute of Metallurgy, Chinese Academy of Sciences,  
Shanghai 200050, P. R. China*

**ABSTRACT** Artificial neural network or pattern recognition together with chemical bond parameters method has been used to classify and predict the characteristics of the phase diagrams of binary molten salt systems. These characteristics are the formability, the chemical stoichiometry, the melting type and the melting point or decomposition temperature of intermediate compound and the formability of solid solution or eutectic mixture. The molten salt systems studied are some halide compounds such as  $\text{MeX-Me}'\text{X}$ ,  $\text{MeX-REX}_3$  and  $\text{MeX-Me}'\text{X}_4$  ( $\text{Me}$ ,  $\text{Me}'$  denote metallic elements, RE rare earth, X halogen) systems. The mathematical models obtained from the experimental data of the known phase diagrams were used to predict the properties of the unknown phase diagrams.

**Key words** phase diagram calculation artificial neural network pattern recognition bond parameter  
binary molten salt system

## 1 INTRODUCTION

Molten salt phase diagram research is one of the most important subject in molten salt physical chemistry. It is very important for the selection of molten salt systems in electrometallurgy and other applications. A large number of data has accumulated in this field, but it is not enough yet for the applications of various types, due to the huge number of molten salt systems. So CALPHAD, the technique for phase diagrams calculation based on thermodynamic relations has been invented, it enables us to calculate phase diagrams with many components using the data

of the known binary phase diagrams. This calculation, however, will not appropriate if there exist some intermediate phases, since the chemical stoichiometry, the melting behaviors (congruent or incongruent) and the melting points or decomposition temperatures of these intermediate compounds can not be predicted by this method. Although the CALPHAD method already have been used for calculation, the lack of the known thermodynamic data limits the usage of it. The formation and properties of intermediate compounds are one of the most difficult obstacles for phase diagram prediction, so it is necessary to propose some semi-empirical ways to investigate

① Project 59434040 supported by National Natural Science Foundation of China and Project 863-715-22-01-01 supported by the National Advanced Materials Committee of China Received Jun. 6, 1997; accepted Sep. 28, 1997

the more complicated phenomena of molten salt systems.

It is well known that the thermodynamic functions are decided by inter-ionic potentials which is related to many chemical bond parameters, and it is reasonable to try to use artificial neural network (ANN) or pattern recognition with chemical bond parameters to find the semi-empirical rules based on the known data. In recent years, we have used pattern recognition and ANN with chemical bond parameters as features of inputs to find the regularities of melting behaviors of some binary alloy phases<sup>[1-3]</sup>. In these work, similar techniques were used to study the phase diagrams calculation for binary or ternary molten salt systems.

## 2 THE PRINCIPLE AND METHOD OF COMPUTATION

The formability, the stoichiometry and the melting type of intermediate phase or compound are decided by synthetically influences or restrictions of many chemical bond parameters in halide molten salt system. Pattern recognition or artificial neural network with chemical bond parameters as features of inputs can extract the regularities of the formability, the stoichiometry and the melting type of intermediate compound from the experimental data of the known phase diagrams. Accordingly, the mathematical models obtained from the pattern recognition or the trained ANN can be used to predict the properties of the intermediate compounds of the unknown phase diagrams or unmeasured parts in some phase diagrams. The computerized prediction can guide the discovery and synthesis of some new compounds. The factors affecting the thermodynamics of intermediate compounds are related to following chemical bond parameters: anionic and cationic radii  $r$ , charge numbers  $Z$ , polarizabilities  $\alpha$ , and electronegativities  $\chi$  etc (in halide systems, the polarizabilities of anions  $X$  have linear relation to the radii in general, so we can substitute  $r$  for  $\alpha$ ). These parameters and their functions can be used to investigate some semi-empirical rules of intermediate compounds in some molten salt systems.

In this work we used these parameters to span a multi-dimensional space and find semi-empirical rules from experimental data by pattern recognition in this space. The rules found can be used for computerized prediction. The pattern recognition methods used here are computational methods mapping the patterns in multi-dimensional space to two-dimensional figures, along with some techniques for mapping the two-dimensional figures back to original multi-dimensional space. Sometimes, certain subspace can be also used to find regularities, for example, a  $r_A \sim r_B$  ( $A, B$  denote metallic ions) diagram is often useful for the study of some regularities of the crystal types of intermediate compounds. The principal component analysis (PCA)<sup>[4]</sup> and partial least squares (PLS) method<sup>[5]</sup> of pattern recognition were used in our work.

Artificial neural network is a new type of information processing system based on modeling the neural system structures of human brain<sup>[6]</sup>, it has some remarkable properties such as self-learning and adaptation, a resistance to noise, a high degree of fault tolerance, which make it suitable for nonlinear problems with complex factors. It is powerful in exploiting information from a vast amount of experimental data through learning, and is specially useful for quantitative prediction. The networks consist in general of an input layer, an output layer, and any number of intermediate layers, called hidden layers. Each unit in the network is influenced by those units to which it is connected, the degree of influence being dictated by the values of the links or connections. The overall behavior of the system can be modified by adjusting the values of the connections, or weights, through the repeated application of a learning algorithm. One of the most popular algorithms is the back propagation (BP) algorithm<sup>[6]</sup>.

In our work, a three-layered neural network and back propagation algorithm were used with chemical bond parameters. The transfer function  $f(x)$  is usually a nonlinear function, we selected hyperbolic tangent function as transfer function,  $f(x) = (e^x - e^{-x}) / (e^x + e^{-x})$ . To avoid local minimum, a simulated annealing

technique had been used. All data of phase diagrams used in this paper were quoted from the refs. [7~9], the journal of inorganic chemistry (in Russian) after 1980 and all handbooks (phase diagrams of ceramics) of the American ceramic society, chemical bond parameters from ref. [10]. All computation were performed on the microcomputer of 586 type.

### 3 RESULTS OF COMPUTATION

#### 3.1 The formability of intermediate compound

Seventy three binary  $\text{MeX-Me}'\text{X}$  systems, including  $\text{LiBr-CsBr}$ ,  $\text{LiBr-RbBr}$ ,  $\text{AgCl-CsCl}$ ,  $\text{LiCl-CsCl}$ ,  $\text{LiF-CsF}$ ,  $\text{LiF-RbF}$ ,  $\text{LiI-RbI}$ ,  $\text{AgBr-CsBr}$ ,  $\text{LiCl-CsCl}$ ,  $\text{AgI-InI}$ ,  $\text{AgBr-RbBr}$ ,  $\text{CuBr-KBr}$ ,  $\text{CuI-TlI}$ ,  $\text{AgI-CsI}$ ,  $\text{AgI-KI}$ ,  $\text{CuCl-CsCl}$  and  $\text{AgBr-KBr}$ ,  $\text{NaBr-CsBr}$ ,  $\text{AgCl-KCl}$ ,  $\text{LiBr-KBr}$ ,  $\text{TlBr-LiBr}$ ,  $\text{NaCl-CsCl}$ ,  $\text{LiCl-KCl}$ ,  $\text{NaCl-RbCl}$ ,  $\text{TlCl-NaCl}$ ,  $\text{KF-CsF}$ ,  $\text{NaF-CsF}$ ,  $\text{LiF-KF}$ ,  $\text{NaF-KF}$ ,  $\text{TlF-KF}$ ,  $\text{LiF-NaF}$ ,  $\text{NaF-RbF}$ ,  $\text{TlF-RbF}$ ,  $\text{AgI-NaI}$ ,  $\text{NaI-CsI}$ ,  $\text{LiI-KI}$ ,  $\text{TlI-KI}$ ,  $\text{TlI-NaI}$ ,  $\text{TlI-RbI}$ ,  $\text{TlCl-RbCl}$ ,  $\text{TlCl-LiCl}$ ,  $\text{KBr-CsBr}$ ,  $\text{RbBr-CsBr}$ ,  $\text{NaBr-KBr}$ ,  $\text{KBr-RbBr}$ ,  $\text{TlCl-CsCl}$ ,  $\text{KCl-RbCl}$ ,  $\text{KI-CsI}$ ,  $\text{RbI-CsI}$ ,  $\text{NaI-KI}$ ,  $\text{KI-RbI}$ ,  $\text{AgCl-NaCl}$ ,  $\text{CuCl-NaCl}$ ,  $\text{RbF-CsF}$ ,  $\text{CuCl-LiCl}$ ,  $\text{RbCl-CsCl}$ ,  $\text{CuBr-LiBr}$ ,  $\text{RbCl-CsCl}$ ,  $\text{AgCl-LiCl}$ ,  $\text{AgCl-CuCl}$ ,  $\text{AgI-CuI}$ ,  $\text{AgBr-LiBr}$ ,  $\text{AgBr-NaBr}$ ,  $\text{CuBr-NaBr}$ ,  $\text{NaBr-RbBr}$ ,  $\text{NaCl-KCl}$ ,  $\text{TlCl-KCl}$ ,  $\text{NaI-RbI}$ , were used as the training set for pattern recognition. The electronegativity difference  $\Delta\chi$  ( $\chi_{\text{X}} - \chi_{\text{Me}}$ , definite  $\chi_{\text{Me}} > \chi_{\text{Me}'}$ ) and the difference of ionic charge-radius ratio  $\Delta Z/r$  ( $(Z/r)_{\text{Me}} - (Z/r)_{\text{Me}'}$ ) were used to span a two-dimensional figure. The  $\text{MeX-Me}'\text{X}$  systems can be classified according to their formability of intermediate compound. Fig. 1 illustrates that the representative points of intermediate compound forming systems and those without intermediate compound forming systems distribute in different regions, there is a clear-cut boundary between two kinds of points, and the small  $\Delta\chi$  or large  $\Delta Z/r$  favors to form intermediate compound. Since the larger  $\Delta Z/r$  is, the larger the polarization force difference between  $\text{Me}$  ion and  $\text{Me}'$  ion acting on  $\text{X}$  ion is,  $\text{X}$  tends to close  $\text{Me}$  and to away from  $\text{Me}'$ , so the

coordination numbers of  $\text{Me}$  ion decrease, those of  $\text{Me}'$  ion increase, and a complex anion  $[\text{MeX}_n]^{(1-n)-}$  is easy to form. Finally, the intermediate compound  $\text{Me}'_{n-1}\text{MeX}_n$  can be formed. That is to say, when  $\Delta Z/r$  is large to certain extent, a stable complex anion or intermediate compound can be formed. If the  $\Delta\chi$  is small, the electronegativity of  $\text{Me}$  ion is larger (such as  $\text{Ag}$ ,  $\text{Cu}$  ion) than one of other metallic ion, an appended polarizability effect between  $\text{Me}$  and  $\text{X}$  ion (not including  $\text{F}$  ion) leads to reduction of the distance between them. Moreover, when the radius of  $\text{Me}'$  ion is large the stable ionic crystal which has high coordination and strong electrostatic interaction can be formed. Because the effective radius of complex anion is large relatively, then intermediate compound only forms between halides of  $\text{Li}$ ,  $\text{Ag}$ ,  $\text{Cu}$  ion and halides of  $\text{Rb}$ ,  $\text{Cs}$  ion with large radius. Accordingly, the predicted results of the formability of intermediate compound for  $\text{LiI-CsI}$ ,  $\text{CuBr-RbBr}$ ,  $\text{CuBr-CsBr}$ ,  $\text{CuI-KI}$ ,  $\text{CuI-RbI}$ ,  $\text{CuI-CsI}$  systems which were not reported indicate that they can form intermediate compounds (\* is the predicted point in Fig. 1).

#### 3.2 The stoichiometry of intermediate compound

In the phase diagrams of molten salt systems, sometimes two salts can form more than one intermediate compounds. So the stoichiometry of compound is an important feature in phase diagram.  $\text{MeX-REX}_3$  type molten salt systems usually form intermediate compounds of  $\text{Me}_3\text{REX}_6$ ,  $\text{MeREX}_4$  type. The systems can be classified into two classes: one only forms  $\text{Me}_3\text{REX}_6$ , while other can form  $\text{MeREX}_4$ . We used the known phase diagrams, such as  $\text{LiF-REF}_3$  ( $\text{RE} = \text{Eu} \sim \text{Lu}$ ,  $\text{Y}$ ),  $\text{NaF-REF}_3$  ( $\text{RE} = \text{La} \sim \text{Lu}$ ,  $\text{Y}$ ),  $\text{KCl-RECl}_3$  ( $\text{RE} = \text{La} \sim \text{Lu}$ ,  $\text{Y}$ ,  $\text{Sc}$ ),  $\text{KF-REF}_3$  ( $\text{RE} = \text{Y}$ ,  $\text{La}$ ,  $\text{Pr}$ ,  $\text{Gd}$ ,  $\text{Yb}$ ,  $\text{Eu}$ ,  $\text{Lu}$ ),  $\text{LiCl-RECl}_3$  ( $\text{RE} = \text{Dy} \sim \text{Yb}$ ),  $\text{CsCl-LaCl}_3$ ,  $\text{CsCl-ScCl}_3$ ,  $\text{RbF-REF}_3$  ( $\text{RE} = \text{Y}$ ,  $\text{Gd}$ ,  $\text{Ho}$ ,  $\text{Er}$ ,  $\text{Sm}$ ),  $\text{CsF-REF}_3$  ( $\text{RE} = \text{Ce}$ ,  $\text{Nd}$ ,  $\text{Sm}$ ,  $\text{Gd}$ ,  $\text{Ho}$ ,  $\text{Lu}$ ),  $\text{RbCl-ScCl}_3$ ,  $\text{CsI-ScI}_3$ ,  $\text{RbI-ScI}_3$ ,  $\text{CsI-TmI}_3$ ,  $\text{LiBr-TmBr}_3$ ,  $\text{NaBr-TmBr}_3$ ,  $\text{CsBr-TmBr}_3$ , as training set. Fig. 2 is the linear mapping (princi-

pal component analysis method) from a three-dimensional space spanned by  $r_+$  (radius of Me ion),  $(Z/r)_{3+}$  (ionic charge-radius ratio of rare earth),  $r_-$  (radius of X ion). It illustrates that the representative points of  $\text{Me}_3\text{REX}_6$  or  $\text{MeREX}_4$  type distribute in different regions, and the large radii of Me and X ion, the large ionic charge-radius ratio of rare earth (small radius of RE ion) favor only formation of  $\text{Me}_3\text{REX}_6$  type compounds.

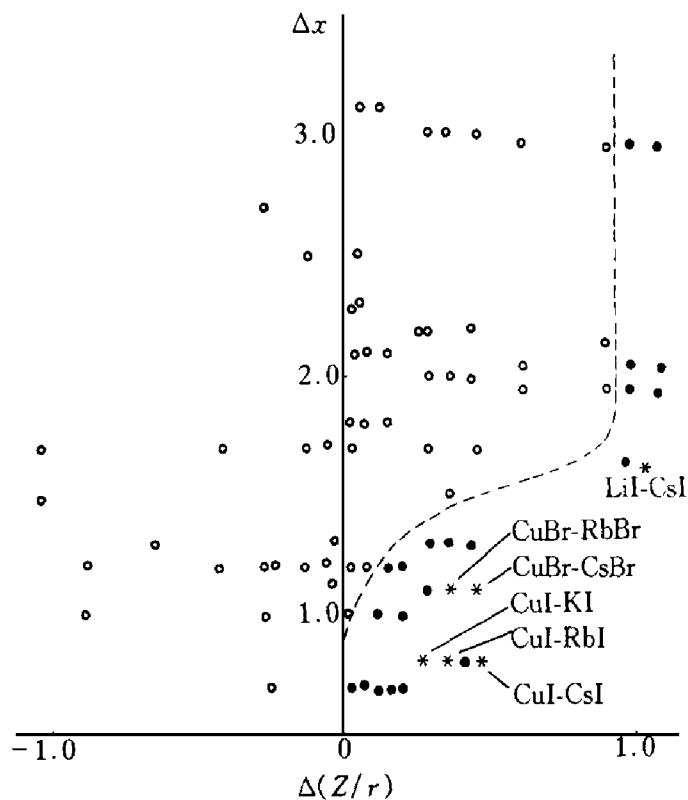


**Fig. 1 Formability of intermediate compound in  $\text{MeX-Me'X}$  systems**

(○—No intermediate compound;  
●—Forming intermediate compound;  
\* —Predicted point)

With the same training set, chemical bond parameters ( $r_+$ ,  $(Z/r)_{3+}$ ,  $r_-$ ) were used as the inputs of ANN, and the stoichiometry data of intermediate compounds were used as the output (output “0” denotes  $\text{Me}_3\text{REX}_6$  type, and “1” denotes  $\text{MeREX}_4$  type compounds). A three-layered neural network (hidden nodes were two) was used to extract useful information. After training, the trained ANN was used to predict the stoichiometry of intermediate compounds of the twelve systems which were not included in

training set and were reported later (J. Inorg. Chem. of Russian after 1984). The predicted output values are as follows:  $\text{RbBr-TmBr}_3$ , - 0.07;  $\text{NaBr-TbBr}_3$ , - 0.04;  $\text{KBr-TbBr}_3$ , - 0.06;  $\text{CsBr-DyBr}_3$ , - 0.07;  $\text{CsBr-HoBr}_3$ , - 0.06;  $\text{NaBr-HoBr}_3$ , - 0.08;  $\text{LiI-HoI}_3$ , - 0.06;  $\text{NaI-SmI}_3$ , - 0.06;  $\text{RbCl-CeCl}_3$ , - 0.07;  $\text{RbI-CeI}_3$ , - 0.03;  $\text{CsF-LuI}_3$ , - 0.04;  $\text{LiF-HoF}_3$ , 1.07. The results of prediction indicate that  $\text{LiF-HoF}_3$  system forms  $\text{Li-HoF}_4$  compound and the other eleven systems form  $\text{Me}_3\text{REX}_6$  type compounds. These predicted results are in agreement with the experimental phase diagrams.

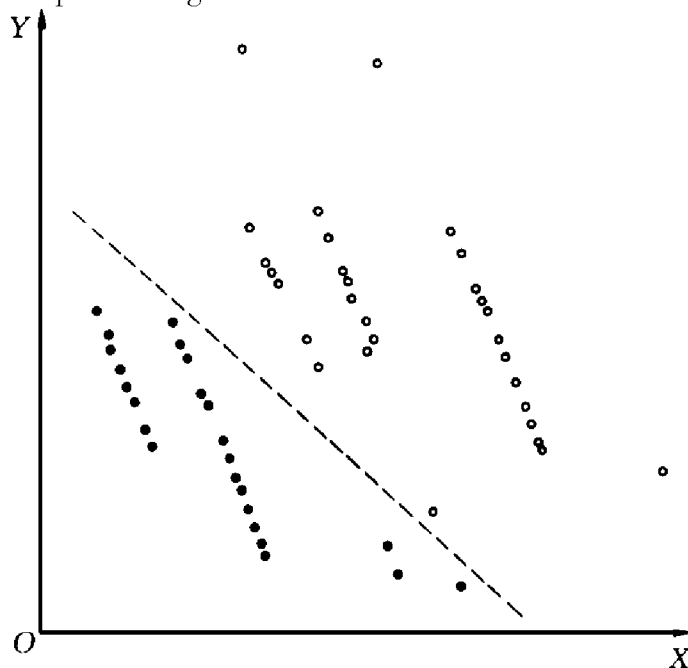


**Fig. 2 Chemical stoichiometry of intermediate compound in  $\text{MeX-REX}_3$  systems**

(○—Forming  $\text{Me}_3\text{REX}_6$  compound;  
●—Forming  $\text{MeREX}_4$  compound;  
 $X = 0.75r_+ - 0.31(Z/r)_{3+} + 0.59r_-$ ;  
 $Y = -0.11r_+ + 0.82(Z/r)_{3+} + 0.56r_-$ )

### 3.3 Melting type of intermediate compound

The congruent melting or incongruent melting of intermediate compound is an important characteristic of phase diagram. The incongruent melting causes peritectic reaction involving the transformation of one crystal lattice into another crystal lattice and a liquid phase. The relative stability of these two lattices (or the difference between the lattice energy) should be a great influence on the occurrence of incongruent melt-

ing. It is well known that there are some factors affecting the lattice energy of ionic crystal such as ionic radii, charge numbers, electronegativities etc. The regularity for distinguishing these two melting types had been investigated by pattern recognition or ANN. We used  $\text{Cs}_2\text{TeBr}_6$ ,  $\text{Cs}_2\text{UBr}_6$ ,  $\text{K}_2\text{TeBr}_6$ ,  $\text{K}_2\text{UBr}_6$ ,  $\text{Na}_2\text{UBr}_6$ ,  $\text{Rb}_2\text{TeBr}_6$ ,  $\text{Rb}_2\text{UBr}_6$ ,  $\text{Tl}_2\text{TeBr}_6$ ,  $\text{K}_2\text{TeCl}_6$ ,  $\text{K}_3\text{ThCl}_6$ ,  $\text{K}_2\text{TiCl}_6$ ,  $\text{K}_2\text{ZrCl}_6$ ,  $\text{Na}_2\text{ThCl}_6$ ,  $\text{Na}_2\text{ZrCl}_6$ ,  $\text{Rb}_2\text{ThCl}_6$ ,  $\text{Tl}_2\text{SnCl}_6$ ,  $\text{Tl}_2\text{TeCl}_6$ ,  $\text{Tl}_2\text{TiCl}_6$ ,  $\text{K}_2\text{SnF}_6$ ,  $\text{Cs}_2\text{TeCl}_6$ ,  $\text{K}_2\text{TiF}_6$ ,  $\text{K}_2\text{TeI}_6$ ,  $\text{Tl}_2\text{TeI}_6$ ,  $\text{Rb}_2\text{SiF}_6$ ,  $\text{Cs}_2\text{TeCl}_6$ ,  $\text{Cs}_2\text{ThCl}_6$ ,  $\text{K}_2\text{PuCl}_6$ ,  $\text{Rb}_2\text{PuCl}_6$ ,  $\text{K}_2\text{SiF}_6$ ,  $\text{Cs}_2\text{TiF}_6$ ,  $\text{Rb}_2\text{TeCl}_6$ ,  $\text{Cs}_2\text{TeI}_6$ ,  $\text{Cs}_2\text{PuCl}_6$ ,  $\text{Rb}_2\text{ZrI}_6$ ,  $\text{Cs}_2\text{ZrI}_6$ ,  $\text{Cs}_2\text{TiCl}_6$ ,  $\text{K}_2\text{SnCl}_6$ ,  $\text{K}_2\text{ZrI}_6$ ,  $(\text{NH}_4)_2\text{TeCl}_6$ ,  $\text{K}_2\text{UCl}_6$ ,  $\text{Li}_2\text{UCl}_6$ ,  $\text{Na}_2\text{UCl}_6$  and  $\text{Cs}_2\text{ZrF}_6$ ,  $\text{K}_2\text{ZrF}_6$ ,  $\text{Na}_2\text{TeF}_6$ ,  $\text{Na}_2\text{UF}_6$ ,  $\text{Na}_2\text{ZrF}_6$ ,  $\text{Na}_2\text{HfF}_6$ ,  $\text{Tl}_2\text{ThF}_6$ ,  $\text{Na}_2\text{ThF}_6$ ,  $\text{K}_2\text{ThF}_6$ ,  $\text{Rb}_2\text{ThF}_6$ ,  $\text{Cs}_2\text{ThF}_6$ ,  $\text{Li}_2\text{TiF}_6$ ,  $\text{Na}_2\text{TiF}_6$  of  $\text{Me}_2\text{Me}'\text{X}_6$  type compounds as training set,  $x_+$  (electronegativity of Me ion),  $r_+$  (Me ionic radius),  $r_-$  (X ionic radius),  $r_{4+}$  (Me' ionic radius) were used to span a four-dimensional space. The  $\text{Me}_2\text{Me}'\text{X}_6$  type compounds are classified according to their melting type (congruent or incongruent melting). Fig. 3 illustrates that the representative points of congruent or incongruent melting distribute in two different regions. Moreover, the result indicates that the large radii of Me and X, or the small radius of Me' favor formation of the  $\text{Me}_3\text{Me}'\text{X}_6$  compounds which are congruent melting type.

If these chemical bond parameters were used as the inputs of ANN, the trained ANN can also be used to predict the melting behavior of  $\text{Me}_2\text{Me}'\text{X}_6$  type compounds, with rather good consistency<sup>[11]</sup>.

### 3.4 The melting point or decomposition temperature of intermediate compound

The melting point (congruent melting) or decomposition temperature (incongruent melting) of intermediate compound is also an important characteristic in phase diagram, but a generally applicable, quantitative method for melting point prediction has not yet been obtained.

Melting process is influenced by many factors described by chemical bond parameters, and ANN is an effective tool for the investigation and prediction of the complicated phenomena affected by many factors, so it would seem reasonable to use ANN-chemical bond parameters method for the prediction of the melting point or decomposition temperature of intermediate compound.

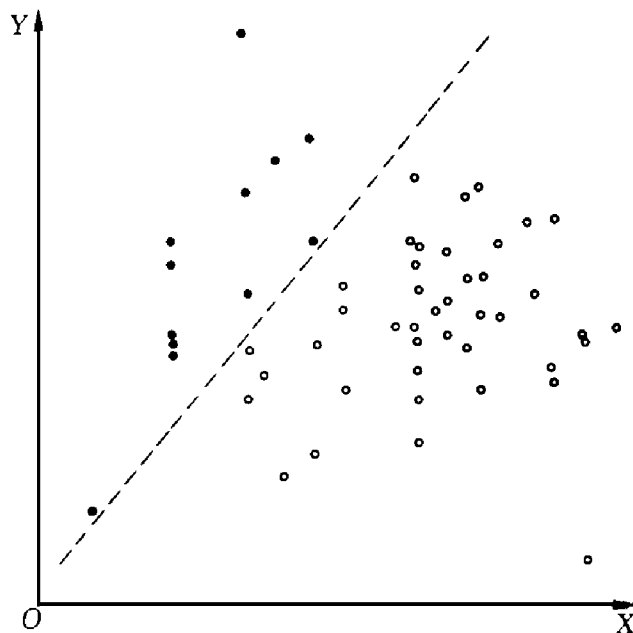


Fig. 3 Melting type of  $\text{Me}_2\text{Me}'\text{X}_6$  compound (PCA method)

(○—Congruent melting; ●—Incongruent melting;  
 $X = 0.05x_+ + 0.50r_+ + 0.86r_- - 0.02r_{4+}$ ;  
 $Y = 0.43x_+ + 0.37r_+ - 0.17r_- + 0.81r_{4+}$ )

We used twenty six melting points of the known  $\text{Me}_3\text{REX}_6$  type compounds as training set, and the  $r_+$ ,  $(Z/r)_{3+}$ ,  $r_-$  as the inputs of a three-layered ANN, the melting points as the output. Hidden nodes were four. After training, the melting points of fourteen compounds which were not included in training set were predicted to test the predicted ability of the adjusted ANN. The training set was  $\text{K}_3\text{RECl}_6$  (RE= Y, La, Ce, Pr, Nd, Sm, Dy, Ho, Yb, Lu),  $\text{K}_3\text{REF}_6$  (RE= Lu, Yb, Gd),  $\text{Cs}_3\text{REF}_6$  (RE= Ce, Sm, Ho, Nd),  $\text{Rb}_3\text{REF}_6$  (RE= Sm, Y),  $\text{Cs}_3\text{CsCl}_6$ ,  $\text{Rb}_3\text{CsCl}_6$ ,  $\text{Cs}_3\text{HoI}_6$ ,  $\text{Rb}_3\text{CsI}_6$ ,  $\text{K}_3\text{CsI}_6$ ,  $\text{Cs}_3\text{TmBr}_6$ ,  $\text{Tl}_3\text{TbBr}_6$ . The testing set was  $\text{K}_3\text{RECl}_6$  (RE= Eu, Gd, Tb, Er),  $\text{K}_3\text{REF}_6$  (RE= Y, Eu),  $\text{Cs}_3\text{REI}_6$  (RE= Tm, Tb, Lu),  $\text{Cs}_3\text{REBr}_6$  (RE= Dy, Ho),  $\text{Cs}_3\text{GdF}_6$ ,  $\text{Rb}_3\text{HoF}_6$ ,

$\text{K}_3\text{GdBr}_6$ . In the same way, 11 incongruent melting compounds were used as the training set for ANN, the decomposition temperatures as the output, hidden nodes were two. The learning set was  $\text{Na}_3\text{RECl}_6$  (RE = Sc, Eu, Gd, Ho, Er, Yb, Lu),  $\text{Li}_3\text{TmBr}_6$ ,  $\text{Na}_3\text{TmBr}_6$ ,  $\text{K}_3\text{TbBr}_6$ ,  $\text{Na}_3\text{TbBr}_6$ . The predicted set was  $\text{Na}_3\text{YCl}_6$ ,  $\text{Na}_3\text{DyCl}_6$ ,  $\text{Na}_3\text{TbCl}_6$ ,  $\text{Na}_3\text{HoBr}_6$ ,  $\text{Na}_3\text{SmI}_6$ .

Fig. 4(a) shows the comparison of the experimental melting point data and the ANN regression or prediction values of the congruently melting of  $\text{Me}_3\text{REX}_6$  compounds, and Fig. 4(b) shows the comparison of the experimental decomposition temperatures and the ANN regression or prediction values of the incongruently melting of  $\text{Me}_3\text{REX}_6$  compounds.

### 3.5 The Classification of continuous solid solution system and simple eutectic mixture

Forty binary MeX-Me'X systems which have no intermediate compound forming, including AgBr-KBr, NaBr-CsBr, LiBr-KBr, TlBr-LiBr, AgCl-KCl, NaCl-CsCl, LiCl-KCl, NaCl-RbCl, TlCl-NaCl, KF-CsF, NaF-CsF, LiF-KF, NaF-KF, TlF-KF, NaF-RbF, TlF-RbF, AgI-NaI, NaI-CsI, LiI-KI, TlI-KI, TlI-NaI, TlI-RbI, TlCl-LiCl, AgCl-RbCl, TlCl-RbCl and

KBr-CsBr, RbBr-CsBr, NaBr-KBr, KBr-RbBr, KCl-RbCl, KI-CsI, RbI-CsI, NaI-KI, KI-RbI, CuCl-NaCl, RbF-CsF, CuCl-LiCl, RbCl-CsCl, AgCl-CuCl, AgI-CuI were used as the training set for pattern recognition. The  $\Sigma r$  (sum of cationic radius),  $|\Delta r|$  (absolute difference of cationic radius),  $|\Delta \chi|$  (absolute difference of cationic electronegativity),  $r_-$  (radius of halogen ion) were used to span a four-dimensional space. The MeX-Me'X systems are classified according to their type of phase diagrams. Fig. 5 indicates that the phase diagrams of continuous solid solution systems and the ones of simple eutectic mixtures distribute in two regions. Computational results illustrate that the small  $|\Delta r|$ , large  $r_-$ , and small  $|\Delta \chi|$  favor formation of the phase diagrams of continuous solid solution; this can be explained as that if the difference of cationic radius increases, the internal strain of lattice will increase when one metallic ion replaces the other, the anionic lattice is destroyed finally, so continuous solid solution can not form. If the electronegativity difference of two metallic ions is large, the crystal types and structures of the two halides are different generally, there is not any geometrical relation in the structures of both [CsCl] or [NaCl] and [ZnS] type, so one

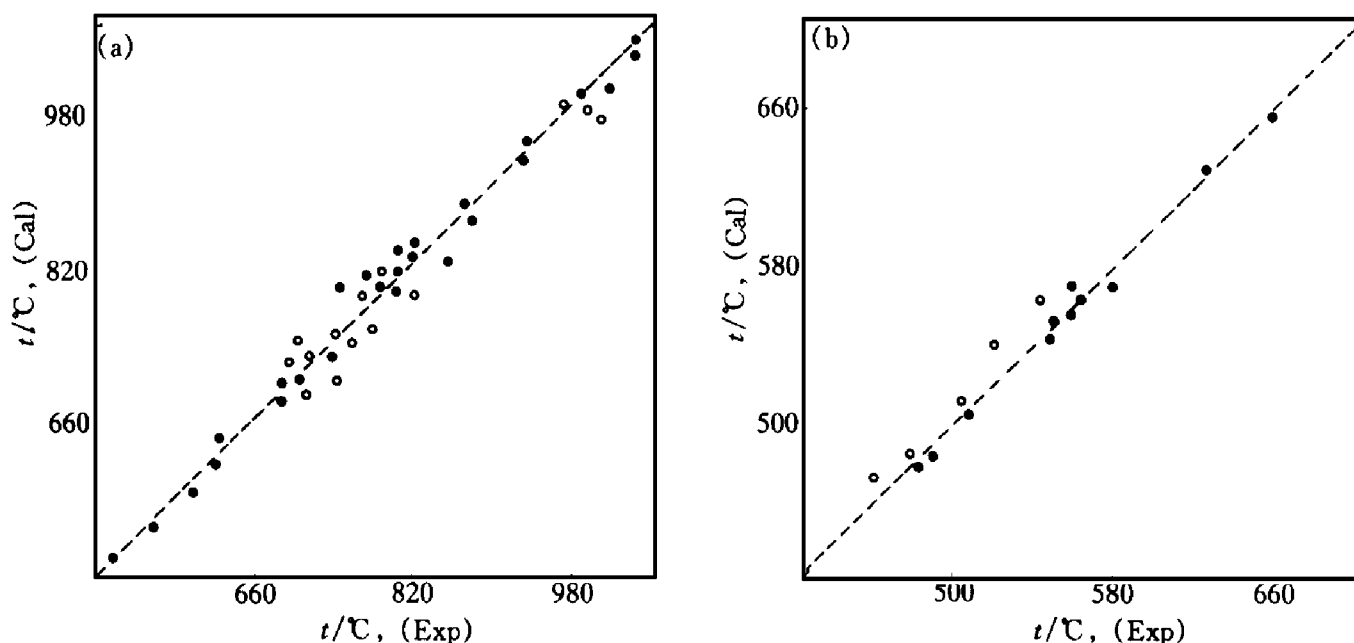
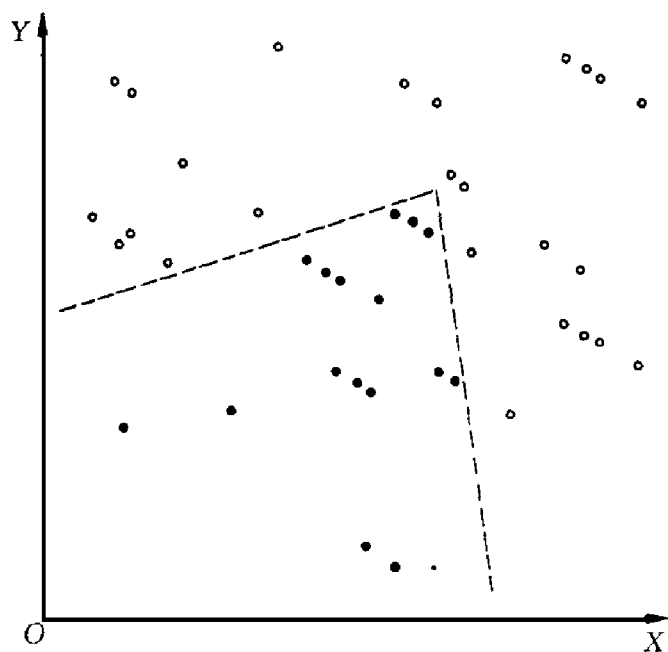


Fig. 4 Calculation of melting point or decomposition temperature of  $\text{Me}_3\text{REX}_6$  type

(a) —congruent melting of  $\text{Me}_3\text{REX}_6$ ; (b) —incongruent melting of  $\text{Me}_3\text{REX}_3$

(● —Training point, ○ —Predicted point)

metallic ion can not substitute continuously for the other in the anionic lattice. If the anionic radius increases, the unit cell of anionic lattice will become large, so the influence of the difference of two metallic ionic radius on the internal strain of lattice will lessen relatively. For example,  $r_K - r_{Na} = 0.35 \times 10^{-10} \text{ m}$ , when X is F ion, the phase diagram of KF-NaF system is a simple eutectic mixture; but X is Br or I, the phase diagram is a continuous solid solution.



**Fig. 5 Formability of continuous solid solution and eutectic mixture (PCA method)**

(○—Eutectics; ●—Solid solution;

$$X = -0.16\Sigma r + 0.75|\Delta r| - 0.62|\Delta X| - 0.18r_-;$$

$$Y = 0.55\Sigma r + 0.61|\Delta r| + 0.57|\Delta X| + 0.07r_-)$$

Therefore, if some suitable chemical bond parameters are selected, the pattern recognition or ANN-chemical bond parameters method can be used to predict or estimate the rules or properties, including the formability, the chemical stoichiometry, the crystal type, the melting behavior, the melting point or decomposition tempera-

ture of intermediate compound, and the formability of continuous solid solution and eutectic system. In addition, ANN method with chemical bond parameters as inputs can estimate the properties as follows<sup>[11]</sup>: the composition and the melting point corresponding to the minimum point in minimum solid solution system (only for MeX-Me'X system), the composition and melting point at eutectic point in eutectic system (for no intermediate compound forming system), the composition at the peritectic point of peritectic reaction.

## REFERENCES

- 1 Chen Nianyi, Li Chonghe, Yao Shuwen *et al.* J of Alloys and Compounds, 1996, 234: 125.
- 2 Chen Nianyi, Li Chonghe, Yao Shuwen *et al.* J of Alloys and Compounds, 1996, 234: 130.
- 3 Li Chonghe, Kang Deshan, Qin Pei *et al.* Trans. Nonferrous Met. Soc. China, 1995, 5: 36.
- 4 Jolliffe I T. Principal Component Analysis. New York: Springer Verlag, 1986.
- 5 Geladi P and Kowalski B R. Anal Chim Acta, 1986, 185: 1.
- 6 Lippmann L P. IEEE ASSP Magazine, 1987, 4: 4.
- 7 Коршунов В Г. Фазовые Равновесия в Галогенидных Системах. Москва: Издательство Металлургия, 1979.
- 8 Воскре сенека я Н К. Справочник по Плазности Систем из Безводных Неорганических Со лейи, Том1, Москва: Издательство АН СССР, 1961.
- 9 Levin E M and McMurdie H F. Phase Diagrams of Ceramic. New York: The American Ceramic Society Inc, 1975.
- 10 Chen Nianyi. Chemical Bond Parameters and Their Applications, (in Chinese). Beijing: Science Press, 1976.
- 11 Wang Xueye. PhD Dissertation, (in Chinese). Shanghai: Shanghai Institute of Metallurgy, Chinese Academy of Sciences, 1996.

(Edited by Wu Jiaquan)